

Effect of morphology on the phonon thermal conductivity of Si, Ge, and Si/Ge core/shell nanowires

© I.I. Khaliava¹, A.L. Khamets¹, I.V. Safronov², A.B. Filonov¹, D.B. Migas^{1,3,¶}

¹ Belarusian State University of Informatics and Radioelectronics,
220089 Minsk, Belarus

² Belarusian State University,
220030 Minsk, Belarus

³ National Research Nuclear University „MEPhI“,
115409 Moscow, Russia

¶ E-mail: migas@bsuir.by

Received December 1, 2021

Revised March 2, 2022

Accepted March 21, 2022

An additional factor in reducing thermal conductivity for thermoelectric applications of semiconductor nanowires is a change in morphology. In this paper, for Si, Ge and core/shell Si/Ge nanowires the effect of the volume fraction and the type of core material on thermal conductivity at 300 K is investigated by means of nonequilibrium molecular dynamics. Nanowires with experimentally observed $\langle 100 \rangle$, $\langle 110 \rangle$, $\langle 111 \rangle$ and $\langle 112 \rangle$ orientations and different cross sections were taken into account. It was found that for $\langle 112 \rangle$ -oriented Si-core/Ge-shell nanowires with a core volume fraction of $\sim 30\%$ the thermal conductivity is the lowest ($5.76 \text{ W}/(\text{m} \cdot \text{K})$), while the thermal conductivity values for pure Si and Ge nanowires are 13.8 and $8.21 \text{ W}/(\text{m} \cdot \text{K})$, respectively.

Keywords: nanowire, core/shell structure, morphology, silicon, germanium, thermal conductivity, molecular dynamics.

DOI: 10.21883/SC.2022.06.53543.9780

1. Introduction

Conversion of heat, emitted by any hot source, for instance the Sun, engine or boiler, directly into electricity is the basis of thermoelectric devices [1]. Efficiency of thermoelectric energy conversion is determined by dimensionless quantity ZT or thermoelectric quality factor determined as $S^2\sigma T/(\kappa_L + \kappa_e)$, where S , σ , T and κ_L , κ_e are respectively the Seebeck coefficient, electric conductivity coefficient, operating temperature and heat conductivity coefficients (phonon/lattice and electronic components) [2]. Electrical conductivity increase is accompanied not only with a rise of electronic heat conductivity, but usually with the Seebeck coefficient decrease, so that it is rather difficult to optimize the resultant value of ZT [2,3].

Efficiency of thermoelectric generators at present is incommensurable with other alternative energy sources, such as solar and fuel cells [4]. Due to this reason, a vital task still is the increase of ZT of thermoelectric materials from 3 and more [2]. Thereat, development of non-toxic and inexpensive thermoelectric materials is considered as a key objective for future commercial applications: many promising thermoelectric materials were studied, for instance, Cu-based, lead-free SnTe, as well as Si and Ge [4]. The latter two are of particular interest, since they form a basis for a well-developed silicon technology. However, due to the high thermal conductivity values, the conventional bulk Si and Ge ($130\text{--}150 \text{ W}/(\text{m} \cdot \text{K})$ [5] and $50\text{--}60 \text{ W}/(\text{m} \cdot \text{K})$ [6], respectively, at 300 K) have a low thermoelectric efficiency.

Special attention at present is paid to low-dimensional semiconductor materials, such as semiconductor nanowires (1D), thanks to their low thermal conductivity [7–9] and rather a high mobility of charge carriers [10,11]. The Si nanowires feature considerable anisotropy of thermal conductivity depending on structure growth direction, while the lowest thermal conductivity is typical of the $\langle 111 \rangle$ orientation as compared to the $\langle 100 \rangle$ and $\langle 110 \rangle$ orientations [12]. A considerable impact of morphology on heat transport in $\langle 100 \rangle$ -oriented square gross section Si nanowires was demonstrated in [13], thermal conductivity is the highest if $\{110\}$ facets are present, and the lowest if $\{170\}$ facets are present. Numerical estimates of thermal conductivity for $\langle 100 \rangle$ -oriented Si and Ge nanowires (~ 20 and $\sim 10 \text{ W}/(\text{m} \cdot \text{K})$ respectively [14]) were by almost an order smaller than for bulk materials. Such a decrease can be due to the phonon scattering from the nanostructure surface (with diameters smaller than the mean free-path of phonons in a homogeneous material). Additional phonon scattering can be achieved on the interface in layered structures or in core/shell structures. It was shown that Si/Ge nanowires of the core/shell type can be made by chemical vapor deposition with a change in synthesis conditions by blocking the axial growth and activating the radial growth [15].

Mainly $\langle 100 \rangle$ -oriented Si/Ge nanowires of the core/shell type with round [14,16] and square [14,17,18] cross-sections were considered in literature as an object for modeling by the molecular dynamics method. The $\{100\}$ [14,18], or $\{110\}$ facets [17] were used for square cross section

Si/Ge nanowires. The surface reconstruction was not implemented on the surface in case of a round cross-section [14,16]. The results given in [14] show that κ_L of square gross section nanowires is smaller than that of round gross section ones. The research of heat transport in $\langle 110 \rangle$ Si square and round gross section nanowires (the facets are not indicated), as well as pentagonal gross section ones (only if twins are formed inside nanowires) has shown that κ_L can be 3 times different, while its smallest values are achieved with a pentagonal cross-section [19]. The $\langle 111 \rangle$ Si nanowires with a saw-tooth like surface morphology (the faces on the surface are not parallel to the nanowire axis) with $\{111\}$ and $\{113\}$ facets or with $\{111\}$ and $\{100\}$ facets featured a 13% or 33% decrease of κ_L as compared to the Si nanowires with the same cross-sectional size and with $\{112\}$ facets [20]. The research of impact of twins density on thermal conductivity of $\langle 112 \rangle$ -oriented square gross section Si nanowires with $\{111\}$, $\{110\}$ facets has found that this effect does not depend on phonon-surface scattering in nanowires with and without such defects, i.e. impact is determined by phonon-interface scattering as in a bulk with twins [21].

The methods of molecular dynamics and tight binding during estimation of ZT for $\langle 110 \rangle$ - and $\langle 111 \rangle$ -oriented Si and Ge-core/Si-shell nanowires with $\{100\}$, $\{110\}$ and $\{111\}$ facets (for the $\langle 110 \rangle$ orientation) and with $\{110\}$ facets (for the $\langle 111 \rangle$ orientation) have established the possibility to reach values > 2 if the surface is considerably rough [22]. Thereat, hydrogen passivation was performed in order to eliminate dangling bonds on the nanowire surface. A similar surface morphology was used in [23] when investigating thermoelectric properties taking into account only the electron component of thermal conductivity of $\langle 110 \rangle$ Ge-core/Si-shell nanowires by means of the ab initio method and taking into account the Boltzmann kinetic equation. It was found that hydrogen passivation of dangling bonds on the surface causes the 2 times increase of ZT at 300 K as compared to the variant of the common (2×1) reconstruction and passivation of the surfaces of Ge-core/Si-shell nanowires [23].

By taking into account the absence of data obtained by one method for Si, Ge nanowires and Si/Ge nanowires of the core/shell type, it is difficult to estimate the impact of morphology on their thermal conductivity. Since the phonon-surface and phonon-interface scattering directly depend on a certain surface orientation [24–26] and interface [14,17,18], correct account of nanostructure morphology allows for more accurate theoretical prediction of their thermoelectric properties. Thus, this paper is aimed at studying the impact of morphology on phonon thermal conductivity of Si/Ge nanowires of the core/shell type as compared to Si and Ge nanowires which have experimentally observed $\langle 100 \rangle$, $\langle 110 \rangle$, $\langle 111 \rangle$ and $\langle 112 \rangle$ growth directions.

2. Materials and methods

The paper dealt with $\langle 100 \rangle$ -, $\langle 110 \rangle$ -, $\langle 111 \rangle$ - and $\langle 112 \rangle$ -oriented Si and Ge nanowires, as well as Si/Ge nanowires of the core/shell type (Si-core/Ge-shell and Ge-core/Si-shell) with sharp interfaces (exclusive of Si and Ge interdiffusion). The diameter of ~ 5.5 nm was chosen for all nanowires, so that the core and shell transverse sizes were varied within several nm. Nanowire surface morphology was chosen based on the results obtained by ab initio calculation methods [27,28]: the $\{100\}$ and $\{110\}$ facets were used for the $\langle 100 \rangle$ orientation, $\{100\}$, $\{110\}$ and $\{111\}$ facets — for the $\langle 110 \rangle$ orientation, $\{110\}$ and $\{112\}$ facets — for the $\langle 111 \rangle$ orientation and $\{110\}$, $\{111\}$ and $\{113\}$ facets — for the $\langle 112 \rangle$ orientation. The surface for the $\{100\}$, $\{112\}$ and $\{113\}$ faces was reconstructed by creating dimers [27,28]. The shapes of the core and nanowire cross-section were the same.

Total energy of the studied nanowires was minimized by molecular statics implemented in the LAMMPS software package [29], taking into account relaxation and optimization of the atomic structure geometry with a variable supercell. Three-dimensional periodic boundary conditions with a ~ 20 nm vacuum gap in the plane of nanowire cross-section were used. Interatomic interaction for the Si-Ge-system was described by Tersoff potential [30]. This potential was used earlier for thermal conductivity simulation of Si/Ge nanowires [14,16].

The phonon component of thermal conductivity was simulated by the method of non-equilibrium molecular dynamics implemented in the LAMMPS software package [29]. The time step was taken equal to 1 fs. At the first simulation stage, the structures were brought to thermodynamic equilibrium by means of isobaric-isothermal and canonical ensembles for 0.1 ns each at $T = 300$ K. A microcanonical ensemble was used for 1 ns at the second simulation stage to establish thermodynamic equilibrium. Temperature in the layers was monitored and maintained using Langevin thermostats, with introduction of the corresponding damping coefficients which affect the relaxation time vibrations oscillations, due to the different atomic masses. This coefficient is equal to 1.0 for Ge, while for Si it is equal to the ratio of Ge and Si atomic masses (~ 2.586), which corresponds to a higher vibration frequency of a lighter atom. Two thermostats were placed for generation of a temperature gradient in the structures: a cold ($T = 290$ K) and a hot one ($T = 310$ K) at the distance of half the supercell size in the direction of heat flux propagation. The quantity of atoms was approximately equal to ~ 4464 (thickness of ~ 4.1 nm) in order to reduce temperature fluctuations in the thermostat area. It should be noted that when the method of non-equilibrium molecular dynamics is used, the calculated thermal conductivity coefficient depends on the size of the supercell, along which the heat flux propagates, when supercell size is smaller than or comparable to average

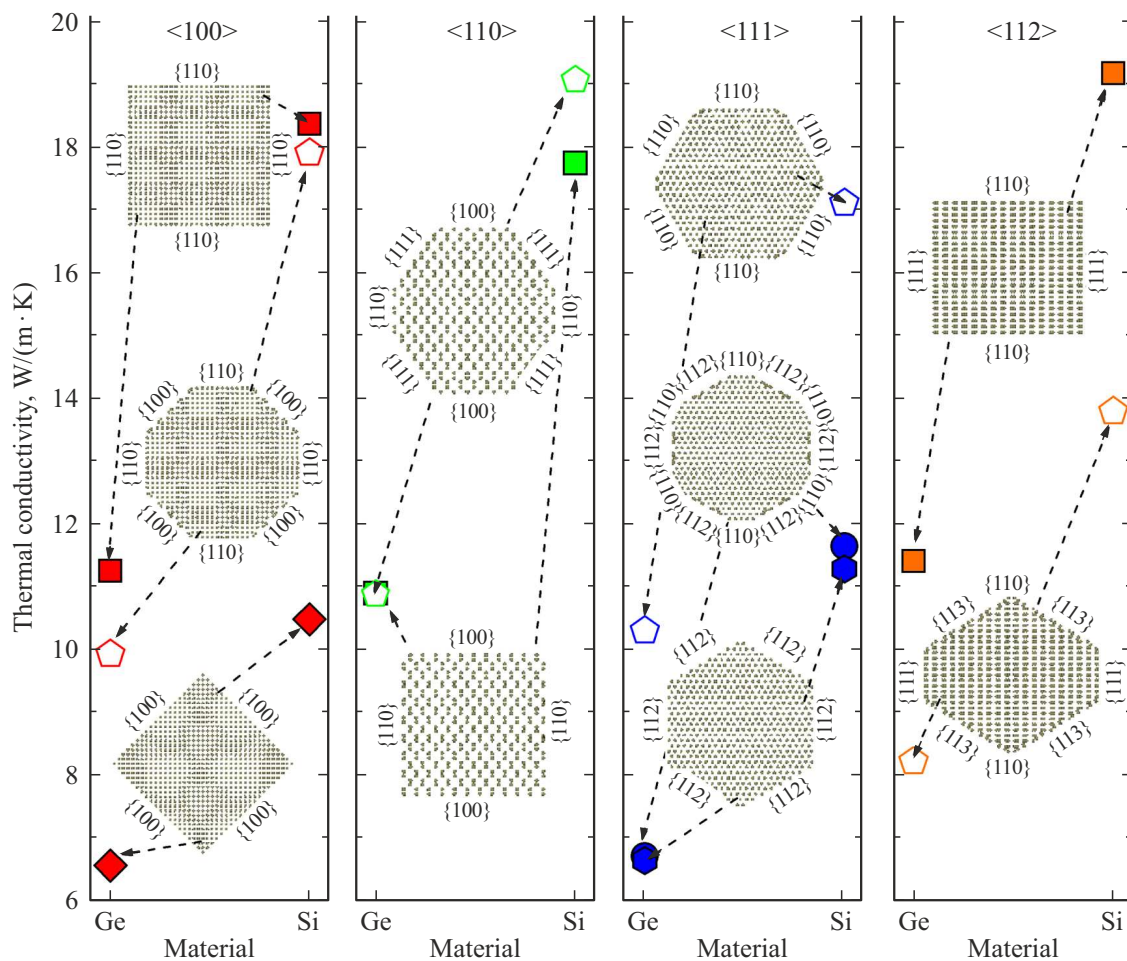


Figure 1. Dependence of thermal conductivity of Ge and Si nanowires having a different orientation and morphology. The corresponding orientations and faces are marked, values of κ_L for each structure are shown with an arrow.

free-path length of phonons at the given temperature. The frequent underestimation (understatement) of thermal conductivity values is eliminated by increasing the supercell size, which requires too much computational effort, but does not significantly affect the thermal conductivity change trends. It is believed that the use of the Fourier law requires the attainment of a linear response regime between reciprocal values of thermal conductivity and supercell length. The authors of [31] conclude that, for instance, the reciprocal value of thermal conductivity for a Si crystal becomes linearly dependent on reciprocal length of the supercell, when the latter reaches sizes of > 100 nm. Taking into account the fact that the average phonon mean free path (ratio of thermal conductivity to heat capacity and average phonon velocity) in a Ge crystal will be smaller than for Si (~ 300 nm [32]), the linear response regime must also be fulfilled in this case with the chosen supercell size. Based on these conclusions, length (L) of all considered Si/Ge nanowires was taken equal to ~ 100 nm. Thermal conductivity coefficient (κ_L) along the nanowire axis was determined from the

Fourier law:

$$\kappa_L = -\frac{E}{2S_{\text{sect}}(dT/dz)},$$

where E — transferred thermal energy; 2 — coefficient related to heat flux propagation in two directions, due to periodic boundary conditions; t — modeling time; S_{sect} — cross-sectional area; dT/dz — temperature gradient in the longitudinal direction. Cross-sectional area was estimated via the ration of the nanowire volume to its height. Nanowire volume was estimated, in its turn, via a sum of atomic volumes.

3. Results and discussion

The use of nanostructures with Si/Ge interfaces, such as multilayer thin films or nanowires of the core/shell type, will not always cause a decrease of κ_L , as was shown for thin Si/Ge films [33]. The formation of a Si/Ge interface inevitably gives rise to an additional phonon scattering mechanism. However, a Si layer is also added, which has a considerably greater κ_L as compared to the Ge layer [33].

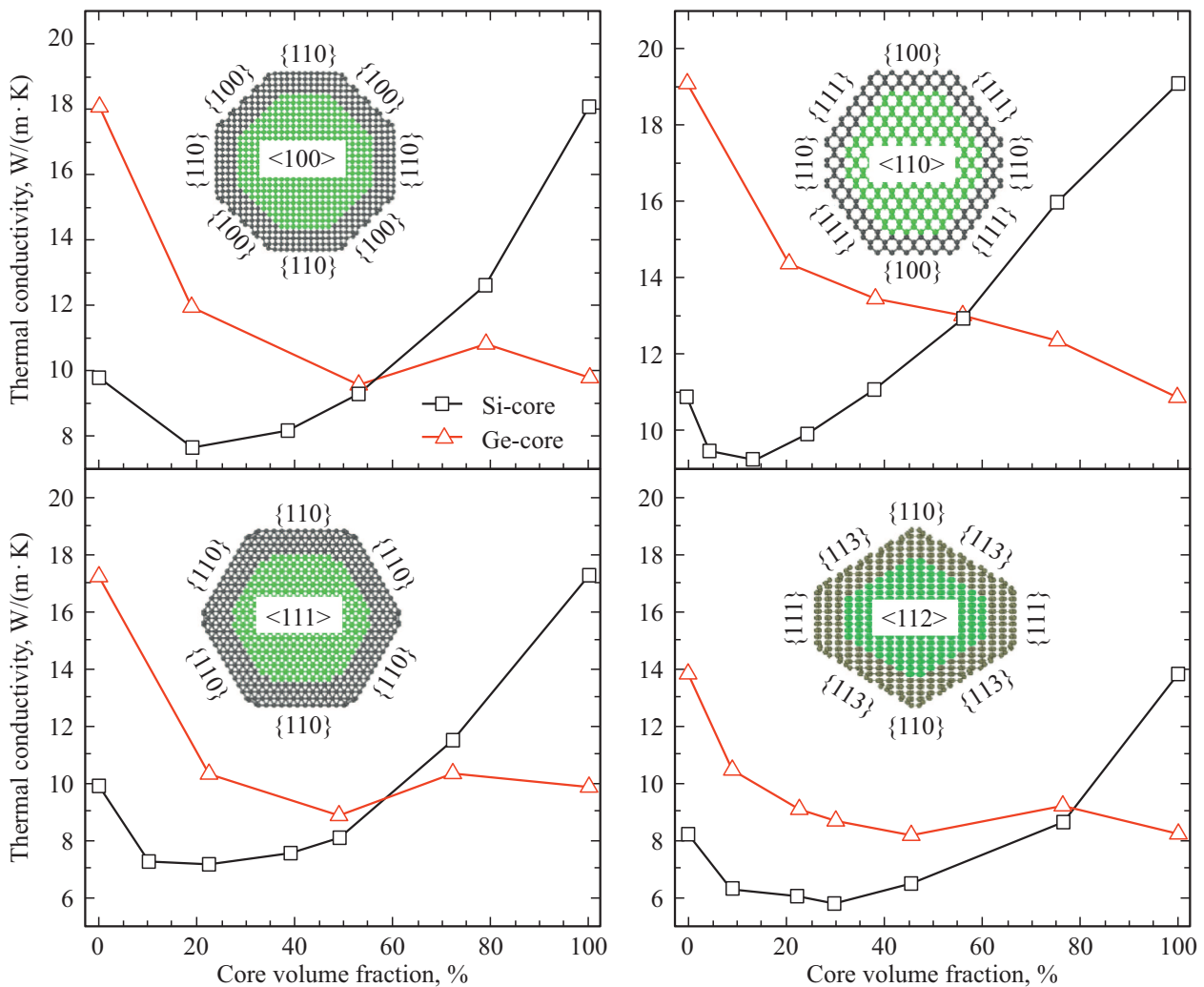


Figure 2. Dependence of thermal conductivity of Si/Ge nanowires of the core/shell type with different orientations on core volume ratio. The inserts show the nanowire morphologies. Legend: Si-core/Ge-shell (square marker) and Ge-core/Si-shell (triangular marker).

Only the heat transfer simulation will help correctly predict a change of κ_L in nanostructures having different surfaces and Si/Ge interfaces.

At the first stage, we studied thermal conductivity of Ge and Si nanowires having a different orientation and morphology of the surface (Fig. 1). The calculation results for the $\langle 100 \rangle$, $\langle 110 \rangle$, $\langle 111 \rangle$ and $\langle 112 \rangle$ orientations clearly show that a change in κ_L values depending on morphology can vary respectively by $\sim 42\%$ ($4.7 \text{ W}/(\text{m} \cdot \text{K})$), $\sim 0.2\%$ ($0.02 \text{ W}/(\text{m} \cdot \text{K})$), $\sim 35\%$ ($3.6 \text{ W}/(\text{m} \cdot \text{K})$) and $\sim 28\%$ ($3.2 \text{ W}/(\text{m} \cdot \text{K})$) in case of Ge nanowires and $\sim 43\%$ ($7.9 \text{ W}/(\text{m} \cdot \text{K})$), $\sim 7\%$ ($1.3 \text{ W}/(\text{m} \cdot \text{K})$), $\sim 34\%$ ($5.8 \text{ W}/(\text{m} \cdot \text{K})$) and $\sim 28\%$ ($5.4 \text{ W}/(\text{m} \cdot \text{K})$) in case of Si nanowires. This effect can be due to a different contribution made by the surfaces to phonon scattering. Indeed, as was shown for thin Si films [25], the surface Si(100) most intensively scatters phonons as compared to other surfaces, this is also inherent in Si nanowires [13,20]. In our case, the $\langle 100 \rangle$ -oriented Si and Ge nanowires with $\{100\}$ facets on the surface have the lowest values of κ_L (Fig. 1). It is also

evident that the $\{112\}$ and $\{113\}$ facets are characterized by effective phonon scattering ($\langle 111 \rangle$ and $\langle 112 \rangle$ orientations). On the other hand, the formation of $\{110\}$ and $\{111\}$ facets leads to an increase of κ_L .

Since the Tersoff potential does not allow for describing the redistribution of electron density and electronic effects, related to reconstruction of surface atoms, κ_L of Si/Ge nanowires of the core/shell type should be studied with account of morphologies (see the inserts in Fig. 2) predicted based on results of nanowire stability calculations by ab initio methods [27,28]. The second stage of our research included simulation of κ_L of $\langle 100 \rangle$ -, $\langle 110 \rangle$ -, $\langle 111 \rangle$ -, $\langle 112 \rangle$ -oriented Si/Ge nanowires of the core/shell type from the volume ratio and core material type (Fig. 2). It will be recalled that the calculated values of κ_L for nanowires made of pure Ge and Si vary respectively from ~ 8 to $\sim 11 \text{ W}/(\text{m} \cdot \text{K})$ and from ~ 14 to $\sim 19 \text{ W}/(\text{m} \cdot \text{K})$, which is by an order lower than for bulk Ge ($50\text{--}60 \text{ W}/(\text{m} \cdot \text{K})$) [6] and Si ($130\text{--}150 \text{ W}/(\text{m} \cdot \text{K})$) [5] due to intensive phonon-surface scattering. The smallest thermal conductivity value

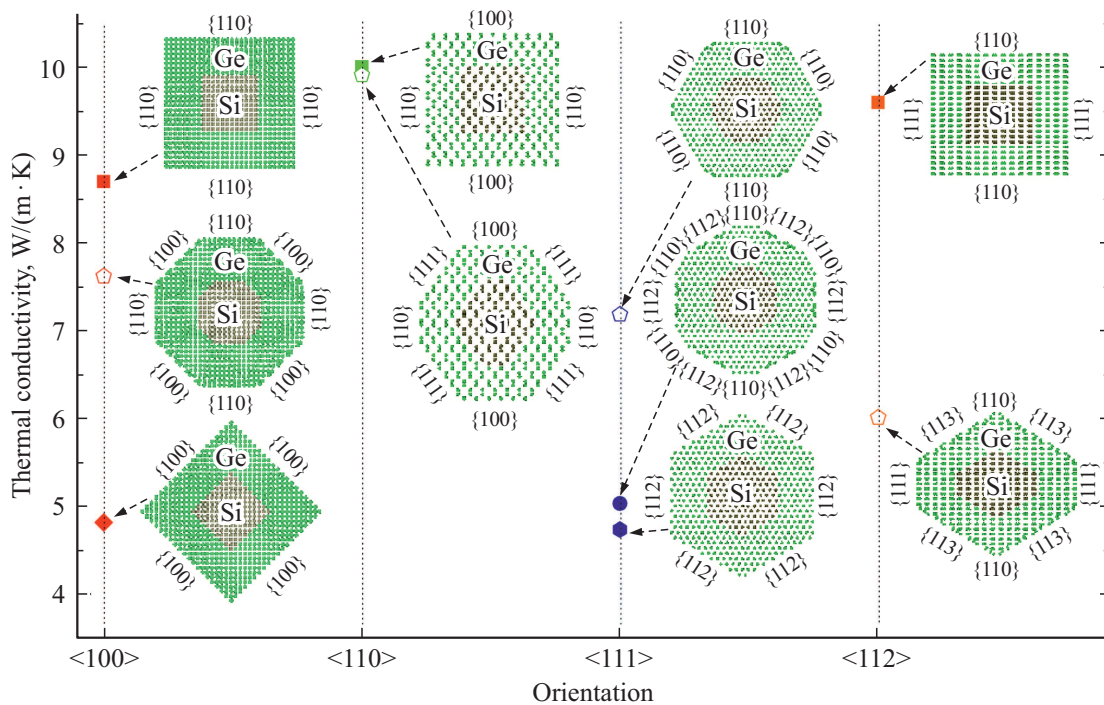


Figure 3. Schematic diagram illustrating the influence of morphology on thermal conductivity of Si-core/Ge-shell nanowires with a different orientation. The corresponding value of κ_L for each structure is shown by an arrow.

is achieved for the Si-core/Ge-shell structure, when the volume ratio of the Si-core is $\sim 10\text{--}30\%$. Thereat, the thermal conductivity value in such nanowires is lower than for Si and Ge nanowires (Fig. 2). Similar trends of κ_L change for $\langle 100 \rangle$ -oriented Si/Ge nanowires of the core/shell type of square and round cross-sections have already been found in [14,16]. Thus, the minimum thermal conductivity value for square gross section nanowires with the volume ratio of the Si-core equal to $\sim 7.4\%$ was $\sim 8 \text{ W}/(\text{m} \cdot \text{K})$, and for round gross section ones it was $\sim 9.5 \text{ W}/(\text{m} \cdot \text{K})$, the volume ratio of the Si-core being $\sim 40\%$ [14], which is close to the values shown in Fig. 2. The obtained results also agree qualitatively with the results of earlier research [17], which show a considerable decrease of κ_L for the $\langle 100 \rangle$ -oriented square gross section Si nanowires when coated with a Ge-shell having the thickness of 1–2 lattice parameter. A distinct trend of thermal conductivity change in relation to growth direction was also established: $\kappa_L^{(110)} > \kappa_L^{(100)} > \kappa_L^{(111)} > \kappa_L^{(112)}$. For instance, these values in the vicinity of the minimum for the Si-core/Ge-shell structure are equal to 9.22, 7.62, 7.18 and 5.76 $\text{W}/(\text{m} \cdot \text{K})$ respectively, and to 19.0, 17.9, 17.1, 13.8 $\text{W}/(\text{m} \cdot \text{K})$ for Si nanowires.

The obtained dependences in Fig. 2 can be explained by several reasons [14], in addition to phonon-surface scattering: different thermal conductivity for Si and Ge, impact of phonon scattering by longitudinal Si/Ge interfaces and coherent phonon resonance. A coherent phonon resonance in core/shell nanostructures is conditioned by a strong coupling between transverse and longitudinal modes

of phonons due to their different velocities in the Si and Ge layers on the interface [18]. This leads to lattice deformations near the phase interface and, as a result, to coupling of these modes, i.e. transverse modes cannot propagate along the nanowire growth direction, which reduces its thermal conductivity. For the Si-core/Ge-shell structure, the contribution made by the Si core (with volume ratio of $\sim 20\%$) to thermal conductivity (taking into account $\kappa_L^{\text{Si}} > \kappa_L^{\text{Ge}}$) is still insufficient to compensate the phonon scattering at the Si/Ge interface and the influence of the coherent phonon resonance effect (Fig. 2). Thus, despite the presence of Si core with large κ_L in the nanowire structure, nanostructure thermal conductivity decreases. It is evident that an increase in core volume ratio (from $\sim 20\%$ and more) leads to a decrease of the ratio of the core surface area to its volume, therefore the effect of phonon scattering on the longitudinal interfaces decreases [14]. For the Ge-core/Si-shell structure, with an increase of the core volume ratio, the contribution made by the Ge core and the effects of phonon-interface scattering and coherent phonon resonance are codirectional towards decrease of κ_L of the nanowire, therefore a dependence without a pronounced minimum is observed here (Fig. 2). Possibly, when the contribution by the Si shell to nanowire thermal conductivity does not compensate the effects of phonon-interface scattering and coherent phonon resonance, the curve of κ_L vs. core volume ratio will have a shallow minimum, as in [14]. It should be emphasized that our nanowires have a more complex morphology, therefore the ratio of core facet dimensions will also change when the core volume ratio

varies. The latter will affect the intensity of phonon-interface scattering and, respectively, the thermal conductivity value, which additionally complicates the interpretation of the obtained results. It should be noted that phonon-surface scattering will chiefly affect the thermal conductivity of the shell whose contribution becomes insignificant with decrease of its thickness. Taking into consideration the anisotropy of thermal conductivity and group velocity of phonons (v_{ph}) in Si nanowires ($\kappa_L^{\langle 110 \rangle} > \kappa_L^{\langle 100 \rangle} > \kappa_L^{\langle 111 \rangle}$ and $v_{\text{ph}}^{\langle 110 \rangle} > v_{\text{ph}}^{\langle 100 \rangle} > v_{\text{ph}}^{\langle 111 \rangle}$ [12]), we may assume that thermal conductivity in Si/Ge nanowires of the core/shell type will be also predominantly affected by group velocity of phonons, as in homogeneous nanowires.

As has been shown earlier, the Si-core/Ge-shell nanowires have the smallest thermal conductivity values when the core volume ratio is $\sim 10\text{--}30\%$ (Fig. 2). At the third stage, we will consider how morphology — not only facets on the surface, but also interfaces of Si/Ge having a different orientation — affects κ_L for Si-core/Ge-shell nanowires. Evidently, the formation of $\{100\}$, $\{112\}$ and $\{113\}$ facets and the corresponding Si/Ge interfaces reduces the values of κ_L (Fig. 3), as in the case of homogeneous nanowires (Fig. 1). The $\{110\}$ and $\{111\}$ facets and the corresponding Si/Ge interfaces less efficiently scatter phonons (Fig. 3). A change in values of κ_L can reach $\sim 45\%$ ($3.9\text{ W}/(\text{m}\cdot\text{K})$), $\sim 0.9\%$ ($0.1\text{ W}/(\text{m}\cdot\text{K})$), $\sim 34\%$ ($2.5\text{ W}/(\text{m}\cdot\text{K})$) and $\sim 37\%$ ($3.6\text{ W}/(\text{m}\cdot\text{K})$) respectively for the $\langle 100 \rangle$, $\langle 110 \rangle$, $\langle 111 \rangle$ and $\langle 112 \rangle$ orientations.

4. Conclusion

The method of non-equilibrium molecular dynamics was used to study the influence of surface morphology on phonon thermal conductivity of Si, Ge nanowires, as well as Si/Ge nanowires of the core/shell type with $\langle 100 \rangle$, $\langle 110 \rangle$, $\langle 111 \rangle$ and $\langle 112 \rangle$ orientations. It was found that surface morphology can give rise to a spread in estimates of κ_L up to $\sim 8\text{ W}/(\text{m}\cdot\text{K})$ for homogeneous nanowires at 300 K. The largest decrease of thermal conductivity was found for Si-core/Ge-shell structures due to intensive phonon scattering by the longitudinal Si/Ge interfaces and coherent phonon resonance irrespective of nanowire growth direction. The minimum values of κ_L for them are lower than those for nanowires made of pure Si and Ge, thereat, the minimum thermal conductivity of $5.76\text{ W}/(\text{m}\cdot\text{K})$ is typical for $\langle 112 \rangle$ -oriented Si-core/Ge-shell nanowires, core volume ratio being $\sim 30\%$. The research results show a potential possibility to use Si/Ge nanowires with a core-shell structure in Si- and Ge-based thermoelectric devices. However, a more precise estimation of the efficiency of thermoelectric devices based on the considered structures requires additional research of the power factor, influence of temperature on thermal conductivity, which is a topic for further research.

Funding

The work has been performed under the state scientific program of the Republic of Belarus „Material science, new materials and technologies“. The work has been also supported by the Priority-2030 program of National Research Nuclear University MEPHI.

Conflict of interest

The authors declare that they have no conflict of interest.

References

- [1] F. Dominguez-Adame. Phys. E: Low-Dim. Syst. Nanostructures, **113**, 213 (2019).
- [2] A.F. Ioffe. *Poluprovodnikovye termoelementy* (M.; L., Izd. AN SSSR, 1956) p. 103 (in Russian).
- [3] N.I. Goktas, P. Wilson, A. Ghukasyan, D. Wagner. Appl. Phys. Rev., **5** (4), 041305 (2018).
- [4] L. Yang, Z.-G. Chen, M.S. Dargusch, J. Zou. Adv. Energy Mater., **8** (6), 1701797 (2018).
- [5] W.S. Capinski, H.J. Maris, E. Bauser, I. Silier, M. Asen-Palmer, T. Ruf, M. Cardona, E. Gmelin. Appl. Phys. Lett., **71** (15), 2109 (1997).
- [6] C.J. Glassbrenner, G.A. Slack. Phys. Rev., **134**, A1058 (1964).
- [7] M. Hu, D. Poulidakos. Nano Lett., **12**, 5487 (2012).
- [8] X. Mu, L. Wang, X. Yang, P. Zhang, A.C. To, T. Luo. Sci. Rep., **5**, 16697 (2015).
- [9] J. Samaraweera, J.M. Larkin, K.L. Chan, K. Mithraratne. J. Appl. Phys., **123**, 244303 (2018).
- [10] X. Chen, Z. Wang, Y. Ma. J. Phys. Chem. C, **115**, 20696 (2011).
- [11] M. Shelley, A.A. Mostofi. Europhys. Lett., **94**, 67001 (2011).
- [12] H. Karamitaheri, N. Neophytou, M.K. Taher, R. Faez, H. Kosina. J. Electron. Mater., **42** (7), 2091 (2013).
- [13] Y. Zhou, Y. Chen, M. Hu. Sci. Rep., **6**, 24903 (2016).
- [14] S. Sarikurt, A. Ozden, A. Kandemir, C. Sevik, A. Kinaci, J.B. Haskins, T. Cagin. J. Appl. Phys., **119**, 155101 (2016).
- [15] O. Hayden, R. Agarwal, W. Lu. Nano Today, **3** (5), 12 (2008).
- [16] A. Ozden, A. Kandemir, F. Ay, N.K. Perkgoz, C. Sevik. J. Electron. Mater., **45**, 1594 (2016).
- [17] M. Hu, K.P. Giapis, J.V. Goicochea, X. Zhang, D. Poulidakos. Nano Lett., **11** (2), 618 (2011).
- [18] J. Chen, G. Zhang, B. Li. Nano Lett., **12** (6), 2826 (2012).
- [19] Y. Gao, Y. Zhou, M. Hu. J. Mater. Chem. A, **6**, 18533 (2018).
- [20] F. Sansoz. Phys. Rev. B, **93**, 195431 (2016).
- [21] A. Porter, C. Tran, F. Sansoz. Phys. Rev. B, **93**, 195431 (2016).
- [22] T. Markussen. Nano Lett., **12** (9), 4698 (2012).
- [23] J.-N. Shen, L.-M. Wu, Y.-F. Zhang. J. Mater. Chem. A, **2**, 2538 (2014).
- [24] P. Heino. Eur. Phys. J. B, **60** (2), 171 (2007).
- [25] Z. Aksamija, I. Knezevic. Phys. Rev. B, **82** (4), 045319 (2010).
- [26] H. Karamitaheri, N. Neophytou, H. Kosina. J. Appl. Phys., **113** (20), 204305 (2013).
- [27] D.B. Migas, V.E. Borisenko. J. Appl. Phys., **105**, 104316 (2009).
- [28] D.B. Migas, V.E. Borisenko, Rusli, C. Soci. Nano Converg., **2**, 16 (2015).
- [29] S. Plimpton. J. Comp. Phys., **117**, 1 (1995).

- [30] J. Tersoff. *Phys. Rev. B*, **39** (8), 5566 (1989).
- [31] Y. He, I. Savic, D. Donadio, G. Galli. *Phys. Chem. Chem. Phys.*, **14**, 16209 (2012).
- [32] Y.S. Ju, K.E. Goodson. *Appl. Phys. Lett.*, **74** (20), 3005 (1999).
- [33] A.L. Khamets, I.I. Kholyavo, I.V. Safronov, A.B. Filonov, D.B. Migas. *FTT*, **64** (5), 564 (2022) (in Russian).